# Effect of Electron Scattering on Second Derivative Ballistic Electron Emission Spectroscopy in Au/GaAs/AlGaAs Heterostructures

M. Kozhevnikov,* V. Narayanamurti,* C. Zheng, and Yi-Jen Chiu
*Electrical and Computer Engineering Department, University of California, Santa Barbara, California 93106*

D. L. Smith
*Los Alamos National Laboratory, Los Alamos, New Mexico 87545*
(Received 29 October 1998)

We present a quantitative study of the second voltage derivative (SD) of ballistic electron emission spectra of Au/GaAs/AlGaAs heterostructures to probe the effect of electron scattering on these spectra. Our analysis of the SD spectra shows that strong electron scattering occurs at the nonepitaxial Au/GaAs interface, leading to an experimentally observed redistribution of current among the electron transport channels. We also show that the effects of hot-electron scattering inside the semiconductor modify the spectra and are sensitive to the heterojunction band structure, its geometry, and temperature. [S0031-9007(99)09041-9]

PACS numbers: 72.10.Fk, 73.20.At, 73.40.Kp, 73.50.Gr

Ballistic electron emission microscopy (BEEM), a three-terminal modification of scanning tunneling microscopy, has recently been shown to be a powerful tool for nanometer-scale characterization of the spatial and electronic properties of semiconductor structures. Since the pioneering work of Kaiser and Bell [1], the capability of BEEM to probe the electronic properties of semiconductors on the local scale has been demonstrated for several systems, including Schottky contacts [2–4] and buried heterojunctions [5–7].

The shape of the BEEM spectrum in the threshold region has to be known in order to derive the correct Schottky or heterojunction barrier energies. Several theoretical models were developed to describe the experimental BEEM spectra. Two commonly used models, based on a planar tunneling formalism [8] and on the transverse momentum conservation at the metal-semiconductor (m-s) interface, are the Bell-Kaiser (BK) model [9] and the Ludeke-Prietsch (LP) model [10]. The LP model extends the original BK theory to include the energy-dependent electron mean free path (mfp) in the metal base layer and the quantum mechanical transmission at the m-s interface. Experimentally distinguishing between the BK and LP models is still difficult, because the quantitative difference between them is comparable with the experimental error, and both of them can fit experimental data reasonably well [6,11,12]. Recently, BEEM theory was extended to the case of buried heterostructures [13], where transmission at the heterojunction interfaces in addition to the m-s interface was considered.

The assumption of transverse momentum conservation, made in the above models, is questionable for the case of nonepitaxial m-s interfaces, which are not atomically abrupt. A deviation from the ballistic picture was experimentally observed, e.g., for Au/Si [14], Pd/Si [15], and Au/GaAs [1,6]. To consider electron scattering at the m-s interface, the m-s interface-induced scattering (MSIS) model was proposed in Ref. [16]. In the strong scattering limit, this model was found to describe the absolute magnitude of the experimentally observed BEEM current for Au/GaAs and Au/Si systems. However, since the observed BEEM spectra are a superposition of current contributions from several different transport channels, it is difficult to conclusively extract the different conduction bands contribution directly from the BEEM spectra fitting.

In this Letter, we report on BEEM spectroscopy of carrier transport through Au/GaAs/AlGaAs heterojunctions. The focus of our study is on the second voltage derivative (SD) of the BEEM spectra in an effort to better understand the effect of carrier scattering in the metal, at the m-s interface and in the semiconductor on the BEEM spectra. The SD-BEEM spectra approximately represent the heterostructure transmission coefficient [13]. The SD-BEEM spectrum, therefore, allows a direct measurement of the explicit energetic partitioning of current through the different transport channels.

The GaAs/AlGaAs/GaAs single barrier (SB) structures were grown on $n^+$ (001)-oriented GaAs substrates by molecular beam epitaxy (MBE). The structures consist of a 500 Å undoped GaAs buffer layer, a $p$-type (Be) $\delta$-doped sheet, a 500 Å GaAs spacer layer, a 50 Å $Al_xGa_{1-x}As$ barrier, and a GaAs cap layer. The Be sheet doping concentration of $N_A = 1.2 \times 10^{12}$ cm$^{-2}$ was designed to compensate for band bending leaving a flat band heterostructure in equilibrium at $T = 300$ K. A detailed analysis is presented here for the SB structures with Al compositions of 0.1, 0.2, 0.3, and 0.42. For each Al composition, a pair of samples were grown with different GaAs cap layer thicknesses of 50 and 300 Å. For comparison, we present also results for a 1 $\mu$m undoped GaAs layer grown on $n^+$ GaAs substrate, the reference

  

GaAs sample. To ensure the same doping concentration, the samples were grown consecutively in the same MBE machine. To fabricate diodes for BEEM, Au layers were deposited by thermal evaporation on the GaAs cap layer to form the metal base and indium Ohmic contacts were soldered to the back of the $n^+$ GaAs substrate to form the collector contact. The Au contacts were nominally 1 mm in diameter and 65 Å thick. The details of the fabrication procedure were published elsewhere [6]. The measurements were performed in a Surface/Interface AIVTB-4 BEEM/STM (scanning tunneling microscopy) using a Au tip. Room-temperature experiments were performed in air, while for the lower temperature experiments, the STM head with a sample was immersed in cold He exchange gas in a nitrogen-cooled dewar. The tip-to-base voltage ($V_t$) was varied between 0.7 and 2 V to acquire the collector current ($I_c$) while keeping a constant tunneling current ($I_t$) of 4 nA. A typical BEEM current value is ~40 pA at 0.5 V above the threshold, and a typical noise level is about 0.5 pA. We found for all samples that the magnitude and shape of BEEM spectra were consistent and reproducible both for different areas on the same sample and for different diodes from the same wafer, indicating the high quality of the diodes used in this study. The spectra were typically averaged for several thousand scans to improve the signal-to-noise ratio.

A BEEM spectrum is presented in Fig. 1(a) for the reference GaAs sample. The inset of this figure shows a schematic band diagram of the experiment. The SD spectrum was extracted from the experimental BEEM spectra by numerical differentiation with a 10 meV window, and is shown in Fig. 1(b). One can see clearly pronounced features in the SD-BEEM spectra. We associate these features in the room-temperature SD spectrum with the $\Gamma$ and $L$ conduction minima in GaAs. The absence of a contribution from the $X$ conduction minimum will be discussed later.

To verify the identification of the observed SD-BEEM features with the transport through different conduction bands, a comparison of room-temperature SD-BEEM spectra for five different Al composition SB heterojunctions is shown in Fig. 2. All of the heterostructures studied utilized an undoped GaAs cap layer and the same preparation procedure, providing a uniform Schottky barrier height for the heterostructure experiments. The differences in the BEEM spectra for the various samples are due to the buried heterostructure.

The data presented in Fig. 2 show a clear increase in the BEEM threshold with increasing Al content. One can distinguish two features in the SD spectra for Al = 0.0, 0.1, and 0.2. These two observed features shift towards higher voltages and converge gradually into one peak as the Al concentration increases. This behavior is consistent with the expected reduction of the energy separation between $\Gamma$ and $L$ conduction minima with the increase of the Al content [6,17].

The SD-BEEM spectra show an obvious deviation from model calculations that assume transverse momentum

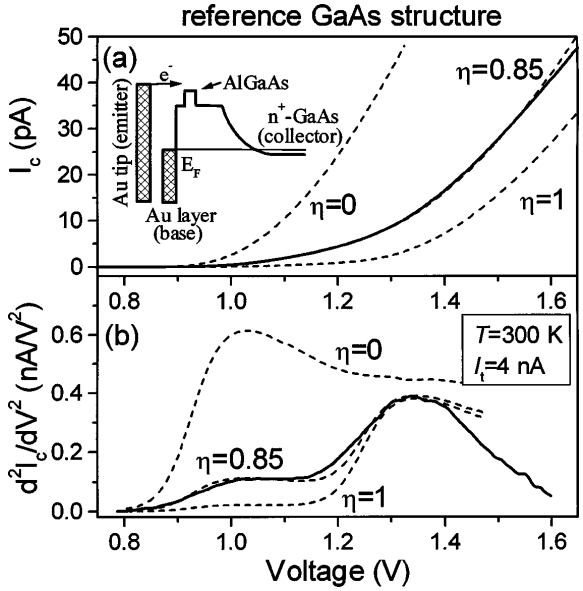


FIG. 1. The room-temperature BEEM (a) and SD-BEEM (b) spectra of the 1-$\mu$m undoped GaAs layer grown on $n^+$ GaAs substrate. The MSIS model calculations (dashed lines) are also presented for three values of $\eta$, the electron scattering probability at the m-s interface. The inset of (a) shows a schematic band diagram of the samples under study.

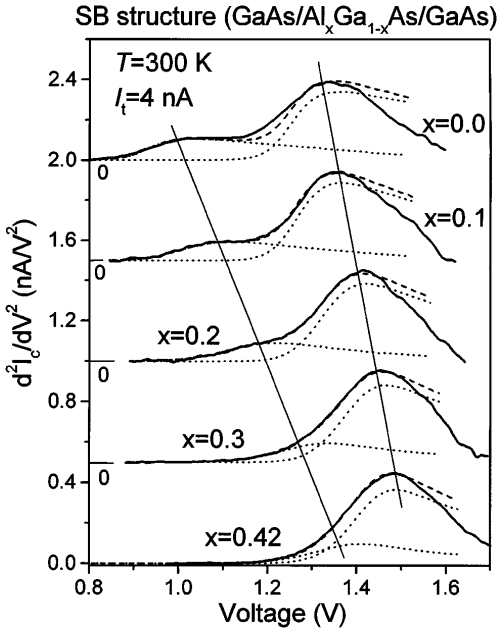


FIG. 2. Room-temperature SD-BEEM spectra for five different Al compositions (solid lines). For clarity, the SD-BEEM spectra are shifted along the vertical axis. Thin solid lines are guides for the eye for the peaks' position development. The MSIS model calculations are also presented. The model calculations show the separate $\Gamma$ and $L$ valley contributions (dotted lines) and their sum (dashed lines).

conservation. Specifically, the $L$-electron collector current is found to be significantly larger than the $\Gamma$-electron collector current, whereas, if transverse momentum conservation is assumed, the contribution of the off-axis $L$ minima can give only a very small BEEM current near the onset, whereas the $\Gamma$ minimum gives a very large BEEM current. A likely explanation for the observed BEEM current due to off-axis valleys is that additional transverse momentum is provided by scattering at the nonepitaxial m-s interface. The possible effect of electron multiple reflection either at the heterostructure interfaces (since this mechanism would amplify mainly the current of the $\Gamma$ electrons which have the longest mfp in the semiconductor heterostructure) or in the metal (the metal layer is thick enough that a multiple reflected component is strongly damped) is small and cannot explain the observed strong $L$-electron transmission and the comparatively weak $\Gamma$-electron transmission.

The small $X$-channel contribution to the SD-BEEM spectra is an unexpected result. One of the three $X$ points projects on the $\Gamma$ direction of the surface Brillouin zone and therefore, independent of whether transverse momentum conservation takes place or not, the contribution of the $X$ electrons to the BEEM current is expected to be large. This result can be explained by electron scattering in the semiconductor. The mfp for the $\Gamma$, $L$, and $X$ electrons near the corresponding threshold energy at $T = 300$ K in GaAs are $\sim$1000, $\sim$100, and $\sim$10 Å [5], respectively. These mfp's decrease with increasing electron energy above threshold. The heterostructure thickness, that is, the combined thickness of the GaAs cap layer and the SB layers is 100 Å. Thus the $X$ electrons contribution to the BEEM spectrum even near threshold will be highly attenuated.

The $X$-channel attenuation may also be influenced by the image potential [11,18]. The Schottky barrier is not spatially abrupt. The image potential results in a lowering of the effective barrier height by $\Delta E_s$ and in the barrier maximum shifting away from the interface toward the semiconductor by a distance $\Delta z$. Taking $N_D = 5 \times 10^{15}$ cm$^{-3}$, $\varepsilon_s = 12$, $E_s = 0.92$ eV at $T = 300$ K for a typical Au/GaAs Schottky contact, we obtain $\Delta E_s \approx 20$ meV and $\Delta z \approx 30$ Å. While the image potential-induced reduction of the effective Au/GaAs Schottky barrier is small, a $\Delta z$ of 30 Å is larger (at 300 K) or comparable (at 85 K) to the expected mfp for the $X$ electrons. The $X$ electrons are scattered in the region between the metallurgical m-s interface and the maximum of the barrier height, and this is temperature dependent.

To experimentally demonstrate that scattering inside the semiconductor structure influences our measurements, we compare the BEEM spectra for pairs of samples with the same Al composition but with cap thickness of 50 and 300 Å. Changing the cap thickness in the range of 50–300 Å should affect mainly the $L$-electron contribution to the BEEM current. The SD-BEEM spectra of the GaAs/$Al_{0.2}Ga_{0.8}$As/GaAs SB samples and the GaAs reference sample are shown in Fig. 3 at $T = 85$ and 300 K. These data are representative of measurements on several pairs of heterostructures. One sees from Fig. 3 that, at $T = 300$ K, the $L$-electron contribution for the sample with a 300-Å-cap layer is reduced by a factor of $\sim$3 as compared with the 50-Å-cap layer sample, whereas the $\Gamma$-electron contribution is about the same for the two samples. One also sees that a new feature due to the $X$-electron contribution shows up in the GaAs reference and the 50-Å-cap layer sample at $T = 85$ K.

The mfp for electrons in GaAs increases with decreasing temperature, since the main scattering mechanism is electron-phonon scattering. As the temperature is decreased from 300 to 85 K, the calculated mfp near the energy threshold increases from $\sim$1000 to $\sim$1500 Å for $\Gamma$ electrons, from $\sim$100 to $\sim$300 Å for $L$ electrons, and from $\sim$10 to $\sim$30 Å for $X$ electrons. This change in mfp is in accord with the temperature dependence of the SD-BEEM spectra shown in Fig. 3. In addition to the spectrum shift expected from the temperature dependence of the energy gap, a strong increase of the signal is observed for the $L$ electrons in the SB sample with the 300-Å-cap layer as the temperature decreases from 300 to 85 K. In addition, one can see in Fig. 3 that the temperature decrease results in the broadening of the high-voltage peak in the SD-BEEM spectrum of the reference GaAs sample. We attribute this broadening with an increased $X$-electron contribution to the collector current, so that the observed high-voltage feature contains contributions from both the $L$ and $X$ transport channels.

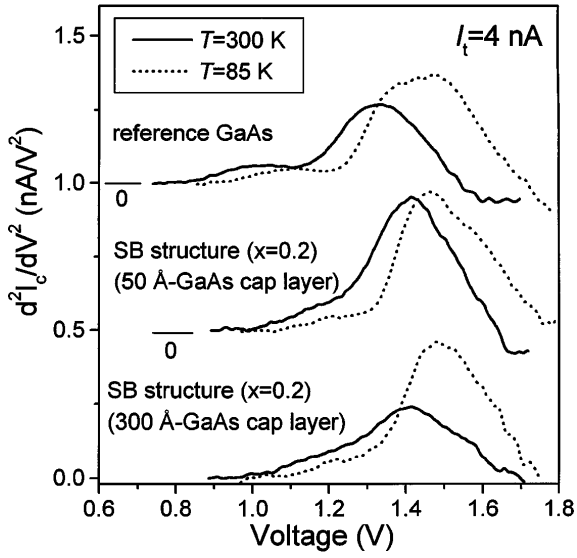


FIG. 3. SD-BEEM spectra for the reference GaAs sample and GaAs/$Al_{0.2}Ga_{0.8}$As/GaAs SB samples with 50 and 300 Å GaAs cap layers, taken at $T = 300$ K (solid curves) and $T = 85$ K (dotted curves). For clarity, the spectra are shifted along the vertical axis.

Figure 1 shows a theoretical fit for the BEEM and SD-BEEM spectra for the reference GaAs sample. We use the MSIS model of Ref. [16], modified to include anisotropy of the electron effective mass in the $L$ valleys, the energy dependence of the electron mfp in the metal base, and finite temperature. (These improvements in the theory lead to a somewhat better agreement with the experimental results, but the difference is not fundamental.) According to the preceding discussion, we neglected any contribution from the $X$ electrons. The MSIS model fit describes the experimental BEEM spectrum reasonably well. The SD-BEEM spectrum clearly separates the contributions from the $\Gamma$ and $L$ electrons; thus, describing the SD-BEEM spectrum quantitatively is a sensitive test of the model. The probability of electron scattering at the m-s interface was adjusted to fit the BEEM and SD-BEEM spectra. These spectra are best described with an 85% probability of the electron scattering at the m-s interface. For comparison, theoretical curves for the cases without scattering and with 100% scattering are also shown.

The MSIS model fits to the SD-BEEM spectra of the SB structures are shown in Fig. 2. The best fits are obtained with the scattering probability at the m-s interface varying between 85% and 92% for the different samples [19]. This small variation in the scattering parameter indicates that our diode fabrication procedure is reproducible and results in approximately the same quality of the m-s interface. Despite the general agreement between the model and the experiment, there is a discrepancy at the high-voltage side of the SD-BEEM spectra; the experimental SD-BEEM spectra decrease more steeply than the calculated ones. This discrepancy is due to scattering in the GaAs and the reduced mfp at higher energy which is not included in the model.

In conclusion, we showed the power of the SD-BEEM spectroscopy in probing the processes affecting the multivalley hot-electron transport in the Au/GaAs/AlGaAs structures. To reliably extract the SD spectra from the original BEEM spectra, both the BEEM current homogeneity and amplitude are important. In contrast to the primary BEEM spectra, the SD-BEEM spectra exhibit explicit energetic separation for the different transport channels. The analysis of the second voltage derivative of the BEEM shows that, while initial electron distribution among the conduction bands of the semiconductor is specified by the m-s interface scattering, with the scattering of the electrons into the $L$ and $X$ valleys at the expense of the ballistic component provided mainly by $\Gamma$ electrons, further electron transport is governed by the difference in the electron mfp for the $\Gamma$, $L$, and $X$ electrons. As a consequence, BEEM can be characterized, in addition to its spatial resolution, by its depth resolution. As the heterostructure, characterized by several transport channels, is buried deeper, the information about these conduction channels is gradually reduced, starting from the transport channel with the shortest electron mfp.

We acknowledge the support of the National Science Foundation under NSF Grant No. ECS 9531133 and the Midwest Research Institute under NREL Contract No. XCR-6-16770. The work of C. Z. was done as part of a collaborative University of California/Los Alamos National Laboratory UCDRC program, and the work of D. L. S. was done while visiting UC Santa Barbara and was conducted under the auspices of the Department of Energy, supported in part by funds provided by the University of California for conduct of discretionary research by Los Alamos National Laboratory.

*Present address: Division of Engineering and Applied Sciences, Harvard University, Cambridge, MA 02138.

[1] W. J. Kaiser and L. D. Bell, Phys. Rev. Lett. **60**, 1406 (1988).
[2] R. H. Williams, Appl. Surf. Sci. **70-71**, 386 (1993).
[3] L. D. Bell, S. J. Manion, M. H. Hecht, W. J. Kaiser, R. W. Fathauer, and A. M. Milliken, Phys. Rev. B **48**, 5712 (1993).
[4] L. D. Bell, A. M. Milliken, S. J. Manion, W. J. Kaiser, R. W. Fathauer, and W. T. Pike, Phys. Rev. B **50**, 8021 (1994).
[5] E. Y. Lee, S. Bhargava, M. A. Chin, and V. Narayanamurti, J. Vac. Sci. Technol. A **15**, 1351 (1997).
[6] J. J. O'Shea, E. G. Brasel, M. E. Rubin, S. Bhargava, M. A. Chin, and V. Narayanamurti, Phys. Rev. B **56**, 2026 (1997).
[7] For review, see, e.g., V. Narayanamurti, Sci. Rep. Res. Inst. Tokohu Univ. A, Phys. Chem. Metall. **44**, 165 (1997).
[8] J. G. Simmons, J. Appl. Phys. **34**, 1793 (1963).
[9] L. D. Bell and W. J. Kaiser, Phys. Rev. Lett. **61**, 2368 (1988).
[10] R. Ludeke and M. Prietsch, J. Vac. Sci. Technol. A **9**, 885 (1991).
[11] M. Prietsch, Phys. Rep. **253**, 163 (1995).
[12] G. N. Henderson, P. N. First, T. K. Gaylord, and E. N. Glytsis, Phys. Rev. Lett. **71**, 2999 (1993).
[13] D. L. Smith and S. M. Kogan, Phys. Rev. B **54**, 10 354 (1996).
[14] L. J. Schowalter and E. Y. Lee, Phys. Rev. B **43**, 9308 (1991).
[15] R. Ludeke, Phys. Rev. Lett. **70**, 214 (1993).
[16] D. L. Smith, E. Y. Lee, and V. Narayanamurti, Phys. Rev. Lett. **80**, 2433 (1998).
[17] S. Adachi, J. Appl. Phys. **58**, R1 (1985).
[18] E. Y. Lee and L. J. Schowalter, J. Appl. Phys. **70**, 2156 (1991).
[19] In Ref. [16] a scattering parameter of unity was used and the $X$-channel contribution was included to describe primary BEEM data on Au/GaAs. Fitting to the SD spectra more precisely defines the model parameters; however, the scattering factor changed by only about 10% (due to the model modification and some sample variations) which does not change the basic picture. Because of the energy range considered, the $X$ channel did not make a large contribution to the calculated results for the direct BEEM data presented in Ref. [16].